J. Meseguer, N. A. Bezdenejnykh, and P. Rodriguez de Francisco

On the Use of Liquid Bridges as Accelerometers

The shape of the interface of a drop of liquid held by surface tension forces between two solid disks, a liquid bridge, depends on the geometry of the supporting disks, the volume of liquid and the external forces acting on the drop. Therefore, once the geometry of the supporting disks and the volume of liquid are fixed, and assuming that the value of the surface tension is known, a way to measure such external forces could be by measuring the deformation of the liquid bridge interface. In this paper the concept of the liquid bridge as a fluid accelerometer that could be used under microgravity conditions to measure very small accelerations is explored. Approximate analytical expressions for the liquid bridge interface and experimental results which support the suitability of the fluid accelerometer concept are presented.

1 Introduction

A liquid bridge, as sketched in fig. 1, consists of an isothermal mass of liquid of density ϱ and surface tension σ, held by surface tension forces between two parallel solid disks, with radii R_1 and R_2. Both disks are a distance L apart. It is also assumed that they can be non-coaxial, $2E$ being the distance between the two axes. The liquid column, of volume V, is subjected to an axial acceleration, g_a, and a lateral acceleration, g_l, with α being the angle between the direction of lateral acceleration and the plane formed by the axes of the disks.

As it is well known, the equilibrium interface shape of a liquid bridge depends on the volume of liquid, V, the geometry of the supporting disks (defined by R_1, R_2, L, and E), the external stimulus (acceleration) and the liquid properties (density and surface tension). Once the volume of liquid and the geometry are fixed, the shape of the liquid bridge interface is uniquely defined by the value of the dimensionless acceleration acting on it. That is, the deformation of the liquid bridge interface depends on the Bond number, a dimensionless parameter that measures the ratio

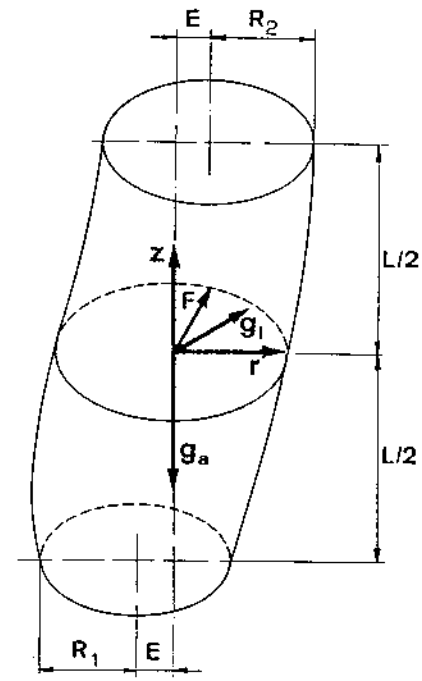

Fig. 1. Geometry and coordinate system for the liquid bridge

of hydrostatic to capillary pressures, $B = \varrho g R_0^2/\sigma$, where $R_0 = (R_1 + R_2)/2$. Therefore, a way to measure the external force acting on the liquid bridge could be by measuring the deformation of the liquid bridge interface, so that a liquid bridge could be used as an accelerometer. Furthermore, since for a given stimulus the deformation of the interface grows as the distance between the disks increases, an accelerometer based on the liquid bridge concept could be adapted to measure in a wide range of small accelerations by varying the length of the liquid column accordingly (but keeping it within the stable length).

In fact, axisymmetric liquid bridges ($E = g_a = 0$) have been used in the past to measure the value of the axial Bond number in experiments performed either on Earth (e.g. *Meseguer* and *Sanz* [1], *Meseguer* et al. [2], *Perales* et al. [3]) and in spacecrafts (*Martinez* [4]). In such papers Bond numbers were calculated by fitting theoretical equilibrium shapes to experimental ones. This comparison between theoretical and experimental equilibrium shapes is not an easy task even in the axisymmetric case because, in general, theoretical equilibrium shapes cannot be analytically ob-

tained; the solution usually adopted has been to calculate approximate expressions for the liquid bridge interface.

In this paper the concept of the liquid bridge as an accelerometer is analyzed. To check the usefulness of the liquid bridge to measure steady accelerations a very simple experimental setup has been developed. This setup allows one to get the contours of a liquid bridge whose axis is oriented at an arbitrary angle with respect to gravitational acceleration. The aim of the experiments is to use the contours of the liquid bridge to calculate the value of the Bond number as well as the orientation of the liquid bridge with respect to the direction of gravity. It must be pointed out that once both axial and lateral Bond numbers are known the calculation of the axial and lateral components of the acceleration involves the use of the value of the surface tension; therefore, the accuracy of the acceleration determination depends on the accuracy of the value of surface tension, which is very sensitive to surface contamination.

The same comment stated above concerning the difficulty of comparing experimental and theoretical liquid bridge contours still holds. Even more, non-axisymmetric liquid bridges are much less studied than axisymmetric ones and leaving apart the early work of *Coriell* et al. [5], only recently non-axisymmetric liquid bridges have been considered (*Perales* [6], *Chen* and *Saghir* [7], *Meseguer* et al. [1], *Laverón-Simavilla* and *Perales* [8]). In the next section an analytical approximation for equilibrium shapes of almost cylindrical liquid bridges is presented as well as details of the data analysis procedure. Experimental setup, results and conclusions are presented in sect. 3.

It must be pointed out that the analytical expression for the liquid bridge interface presented here has been obtained under the assumption that some of the parameters appearing in the problem formulation are very small, particularly the Bond number $B = \varrho g R_0^2/\sigma$. According to this expression there are different ways to obtain low values of the Bond number. One way could be by reducing the value of the acceleration acting on the liquid column, g. However, this requires performing the experiments on board a space-platform or in a sounding rocket. In an Earth-laboratory there are two widely used ways to get low values of Bond number: one of them is by surrounding the liquid bridge with another immiscible liquid of almost the same density (this is the so-called neutral buoyancy technique). In this case ϱ, which is the difference between the density of the liquid bridge and the density of the surrounding medium, can be made, within some limits, as small as desired to get the desired value of the Bond number. The second method used is to reduce the size of the sample, that is the characteristic length R_0. This method is the one used in the experiments described below.

2 Mathematical Model

Let $r = F(z, \theta)$ be the dimensionless equation of the free surface of the liquid bridge (fig. 1). Equilibrium shapes of liquid bridges are described by the Young–Laplace equation, which in dimensionless variables states:

$$M(F) + P - B_a z + B_l F \cos(\theta - \alpha) = 0, \tag{1}$$

where $M(F)$ is the curvature of the interface, defined as

$$M(F) = \{F[1 + (F_z)^2](F_{\theta\theta} - F) + FF_{zz}[F^2 + (F_\theta)^2] - 2F_\theta(F_\theta + FF_zF_{z\theta})\}\{F^2[1 + (F_z)^2] + (F_\theta)^2\}^{-3/2}. \tag{2}$$

The boundary conditions are:

$$F(\pm\Lambda, \theta) = [(1 \pm h)^2 - e^2 \sin^2(\theta)]^{1/2} \pm e \cos(\theta), \tag{3}$$

$$F(z, \theta + 2\pi) = F(z, \theta), \tag{4}$$

$$\int_{-\Lambda}^{\Lambda} \mathrm{d}z \int_0^{2\pi} F^2 \,\mathrm{d}\theta = 4\pi\Lambda V. \tag{5}$$

In the above expressions $F(z, \theta)$ and z have been made dimensionless with $R_0 = (R_1 + R_2)/2$. Other parameters appearing in the problem formulation are the slenderness, $\Lambda = L/(2R_0)$, the dimensionless volume, $V = V/(\pi R_0^2 L)$, the dimensionless eccentricity, $e = E/R_0$, the parameter that measures the difference between the sizes of the disk, $h = (R_2 - R_1)/(R_2 + R_1)$ and the axial and lateral Bond numbers, $B_a = \varrho g_a R_0^2/\sigma$ and $B_l = \varrho g_l R_0^2/\sigma$, respectively, where ϱ is the difference between the densities of the liquid bridge and the surrounding liquid and σ is the surface tension. The constant P appearing in eq. (1) is a constant pressure which has been made dimensionless with σ/R_0. The subscripts z and θ indicate derivatives with respect to z and θ, respectively.

Let us introduce the following parameters: $\varepsilon_1 = v = V - 1$, $\varepsilon_2 = B_a$, $\varepsilon_3 = h$, $\varepsilon_4 = B_l$, $\varepsilon_5 = e$. In the case when $\varepsilon_i = 0$ the problem (1), (3)–(5), has the solution $F(z, \theta) = 1$. If the different parameters ε_i are small enough, $\varepsilon_i \ll 1$, equilibrium shapes could be expressed as

$$F(z, \theta) = 1 + \sum_{i=1}^{5} \varepsilon_i f_i(z, \theta) + \sum_{i=1}^{5}\sum_{j=1}^{5} \varepsilon_i\varepsilon_j f_{ij}(z, \theta). \tag{6}$$

The introduction of this series expansion in the problem formulation gives the following set of problems:

– order ε_i:

$$f_{izz} + f_{i\theta\theta} + f_i + p_i - \Delta_{i2} z + \Delta_{i4}\cos(\theta - \alpha) = 0, \tag{7}$$

$$f_i(\pm\Lambda, \theta) = \pm\Delta_{i3} \pm \Delta_{i5}\cos(\theta), \tag{8}$$

$$f_i(z, \theta + 2\pi) = f_i(z, \theta), \tag{9}$$

$$\int_{-\Lambda}^{\Lambda} \mathrm{d}z \int_0^{2\pi} f_i \,\mathrm{d}\theta = 2\pi\Lambda\Delta_{i1}; \tag{10}$$

– order $\varepsilon_i\varepsilon_j$:

$$f_{ijzz} + f_{ij\theta\theta} + f_{ij} + p_{ij} - f_i f_j + \frac{1}{2} f_{iz} f_{jz} - \frac{1}{2} f_{i\theta} f_{j\theta} - f_i f_{j\theta\theta} - f_{i\theta\theta} f_j + \frac{1}{2(1+\Delta_{ij})}[(1 + \Delta_{i4})\Delta_{j4} f_i + (1 + \Delta_{j4})\Delta_{i4} f_j]\cos(\theta - \alpha) = 0, \tag{11}$$

$$f_{ij}(\pm\Lambda, \theta) = -\frac{1}{2}\Delta_{i5}\Delta_{j5}\sin^2(\theta), \tag{12}$$

$$f_{ij}(z, \theta + 2\pi) = f_{ij}(z, \theta), \tag{13}$$

$$\int_{-A}^{A} \mathrm{d}z \int_{0}^{2\pi} (2f_{ij} + f_i f_j)\, \mathrm{d}\theta = 0. \tag{14}$$

In these expressions above Δ_{ij} stands for the Kronecker delta function ($\Delta_{ij} = 0$ if $i \neq j$ and $\Delta_{ij} = 1$ if $i = j$). The solutions corresponding to the different ε_i and $\varepsilon_i \varepsilon_j$ problems are given in the appendix.

It must be pointed out that the problem solved here is similar to the one presented in [2], although in that paper only axisymmetric configurations were considered ($\varepsilon_4 = \varepsilon_5 = 0$). Therefore the functions f_i, $i = 1, 2, 3$, and f_{ij}, $i, j = 1, 2, 3$ are the same as those obtained in that paper, provided the variables $S = F^2$ is used instead of F (it must be pointed out also that there is a misprint in expression (A.9a) of *Meseguer* et al. [2], in which 1/4 must be replaced with 1/2).

Eq. (6) can be used to calculate the steady acceleration acting on a liquid bridge provided the liquid bridge configuration is close enough to the reference configuration (a cylindrical liquid column between coaxial equal disks). This could be done by fitting eq. (6) to experimental equilibrium shapes by the least square method. However, since eq. (6) is non-linear in ε_i, the resulting system of equations to determine ε_i is highly non-linear, complicating the solution process. Such difficulty can be avoided by spliting the calculation process into two steps. In the first step only the linear part of eq. (6) is considered so that a linear system of equations is obtained, from which the linear-fitting values $\varepsilon_i = \varepsilon_{i0}$ are obtained. Such system of equations is obtained by making $\partial D / \partial \varepsilon_{i0} = 0$, where $D = \Sigma_k (1 + \Sigma_i f_i \varepsilon_{i0} - R)^2$, resulting in the following equations:

$$\sum_j \left(\sum_k f_i f_j \right) \varepsilon_{j0} = \sum_k [(R - 1) f_i], \quad i = 1, 2, \ldots. \tag{15}$$

In which $R = R(z_k, \theta)$ stands for the experimental values of the radius of the interface at coordinates z_k and θ, whereas Σ_k indicates addition with respect to z_k.

In the second step it is assumed that the quadratic-fitting values are close to the linear-fitting ones, such that $\varepsilon_i = \varepsilon_{i0} + \delta_i$, $\delta_i \ll \varepsilon_{i0}$, the new variables being δ_i, which are obtained after neglecting $\delta_i \delta_j$ terms in the new system of equations which results from $\partial D / \partial \delta_i = 0$, taking into account that now the second order expression for F, eq. (6), must be used instead of the linear part. This new system of equations becomes:

$$\sum_j \left[\sum_k (G_i G_j + 2F_m f_{ij}) \right] \delta_j = -\sum_k (F_m G_i), \quad i = 1, 2, \ldots, \tag{16}$$

where

$$G_i = f_i + 2 \sum_m f_{im} \varepsilon_{m0}, \text{ and}$$

$$F_m = 1 + \sum_i f_i \varepsilon_{i0} + \sum_i \sum_j f_{ij} \varepsilon_{i0} \varepsilon_{j0} - R.$$

Before using eq. (6) to calculate accelerations it would be helpful to know the validity range of eq. (6), or at least the error affecting the values of the parameters ε_i obtained. An idea about the errors involved when eq. (6) is used can be obtained by comparing the equilibrium shapes given by eq. (6) with exact ones.

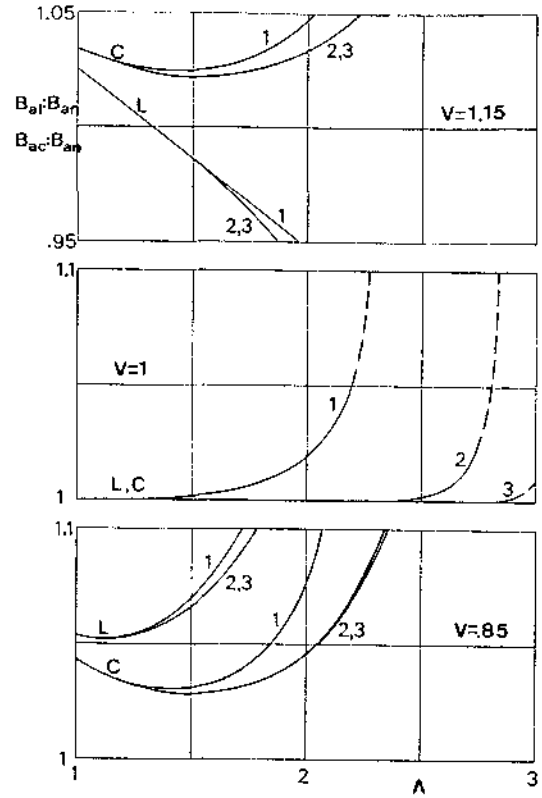

Fig. 2. Variation with the slenderness, Λ, and the volume of liquid, V, of the ratios of calculated axial Bond number to the nominal Bond number, B_{al}/B_{an} and B_{ac}/B_{an}, where the subscript a means axial Bond number and the subscripts l, c and n mean linear fitting, quadratic fitting and nominal value, respectively. Numbers on the curves indicate the value of the exponent n of the nominal Bond number, $B_{an} = 10^{-n}$. Curves labelled with L correspond to B_{al}/B_{an} whereas those labelled with C correspond to B_{ac}/B_{an}. The results correspond to axisymmetric liquid bridges between equal and coaxial disks ($B_t = h = c = 0$)

For axisymmetric liquid bridges ($\varepsilon_4 = \varepsilon_5 = 0$) equilibrium shapes can be numerically calculated by using the shooting method. The fitting method described above has been applied by using such numerically calculated shapes leaving $\varepsilon_2 = B_a$ as the only unknown, so that the axial Bond number resulting from eq. (6) can be compared with the exact one used for numerical computations. The results of this comparison are shown in fig. 2. In this plot the variation with the slenderness Λ of the ratios B_{al}/B_{an} and B_{ac}/B_{an} (where the subscripts l, c and n mean linear fitting, quadratic fitting and nominal value used to calculate numerical equilibrium shapes, respectively) have been represented for several values of the axial Bond number, B_{an}, and different values of the volume, V, for the case of liquid bridges between equal and coaxial disks ($h = c = 0$). In general, a non-linear expression for the liquid bridge interface gives more accurate values of the acceleration than a linear expression, as shown in fig. 2. It must be pointed out that the obtained values of the acceleration are greater than the nominal ones, except in the linear case, where for $V > 1$ the values obtained are greater or smaller than the nominal

ones depending on the slenderness. Note that for each value of the liquid volume and of the nominal Bond number the fitted Bond numbers become unacceptable when Λ is large enough. This is because as Λ increases (or V decreases) the liquid bridge configuration is closer to the corresponding stability limit, and the deformation of the liquid bridge interface grows. This effect is not symmetric with respect to the volume; for a given Λ the error is greater when $V < 1$ than when $V > 1$ for the reason explained above: the error depends on how close to the stability limit the liquid bridge configuration is.

According to fig. 2, the more accurate results are obtained when $V = 1$. In this case, when only axisymmetric liquid bridges are considered, there is no difference between linear and quadratic fitting except close to the corresponding stability limit (when the curves become vertical).

In the non-axisymmetric case the comparison with exact theoretical equilibrium shapes is more difficult (the integration of eq. (1) requires a considerable computing effort [8]. However, some insight can be obtained by analyzing eq. (6). Since eq. (6) is an approximation of the solution of the problem formulation (1)–(5), it will not satisfy eq. (1) exactly or, in other words, P will not be constant. Therefore, any parameter measuring the non-uniformity of the pressure can be a parameter measuring the accuracy of eq. (6) to describe an equilibrium shape. This parameter could be $\Delta P = (P_{max} - P_{min})/\bar{P}$, where P_{max} and P_{min} are the maximum and the minimum of the pressure as given by eq. (1), once F is substituted by eq. (6), and $\bar{P}$ is the average pressure. The variation with both the axial and lateral components of Bond number, B_a and B_l, respectively, of ΔP for a liquid bridge with $\Lambda = 2.44$, $V = 1$, $h = 0$ and $e = 0$, is shown in fig. 3. Note that for a given value of the Bond number, eq. (6) gives more accurate results when only lateral acceleration is considered than in the axisymmetric case.

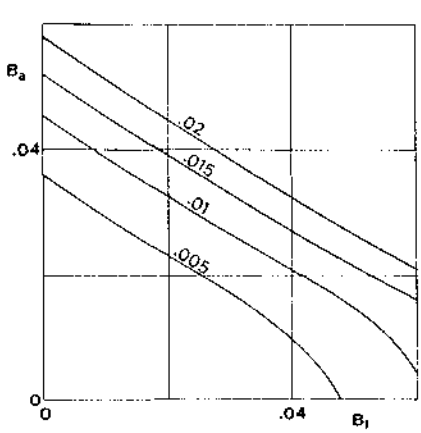

Fig. 3. Dependence of the accuracy of eq. (6) to describe an equilibrium liquid bridge interface on the axial and lateral components of the Bond number, B_a and B_l, respectively. Numbers on the curves indicate the value of the parameter ΔP defined in the text. The results correspond to a liquid bridge with a slenderness $\Lambda = 2.44$, cylindrical volume, $V = 1$, and equal and coaxial disks, $h = 0$, $e = 0$

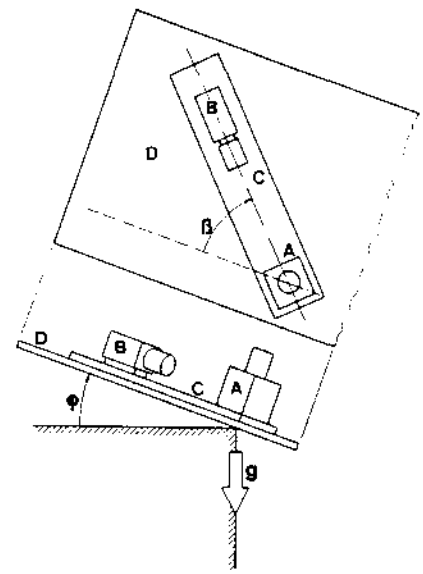

Fig. 4. Sketch of the experimental apparatus: (A) liquid bridge cell, (B) CCD camera, (C) rotating platform, (D) tilting table

3 Experiments

To experimentally check the suitability of liquid bridges to measure accelerations, an experimental facility, as sketched in fig. 4, has been developed. The apparatus consists of a millimetric liquid bridge cell (A) in which a liquid bridge can be formed, and a CCD camera (B), both mounted on a platform (C) which in turn is mounted on a tilting table (D). The platform can be rotated around a fixed point of the tilting table, and its position being measured by the angle β. The tilting table is articulated along an axis to a fixed base, φ being the angle between the tilting table and the fixed base. Other equipment used, but not shown in fig. 4, are a video recorder, a PC computer with an image processor, and a background illumination system.

The liquid bridge cell consists of a three-axis table. The upper disk can be displaced along the z-axis by means of a micrometric screw, with an accuracy of 0.01 mm, whereas the other disk is mounted on a plate that can be displaced parallel to the xy-plane by means of two micrometric screws which allow the displacement of the plate along the x-axis and the y-axis. Both disks have a radius $R_0 = 0.41$ mm, and they are made of calibrated stainless steel tube. Working liquid, distilled water, is injected and removed through a hole in the upper disk connected to a calibrated syringe by flexible tubing. During the experiments the disks were kept coaxial and the distance between them was $L = 2$ mm, so that the slenderness was $\Lambda = 2.44 \pm 0.01$.

A typical experimental sequence is as follows: with the disks at the desired separation, the tilting table D is rotated up to the nominal value of the tilting angle (φ_n), and the platform C, which supports the liquid cell and the CCD camera, is rotated up to the nominal value of the rotating angle (β_n). Then a drop of water is injected between the disks. If the volume of liquid is too large part of the liquid is removed manually through the hole in the upper disk

until a liquid bridge with a volume slightly greater than the cylindrical one is obtained. During the experimental sequence the volume of liquid is continuously decreasing due to evaporation; liquid bridge contours are continuously digitized and the volume of liquid calculated from such contours. When the calculated volume is in the range $V = 1 \pm 0.005$ the liquid bridge contour is saved for further analysis. Then the platform C is rotated up to an angle $\beta_n + \pi/2$ and the same process is repeated again. In this way two perpendicular views of the liquid bridge are obtained. Of course these two views are not of the same liquid bridge but two different liquid bridges of the same slenderness and volume. Obviously to use the liquid bridge as an accelerometer it is needed to record at least two different views of the liquid bridge interface at the same time (preferably perpendicular). This can be done by using a second camera or by placing a mirror on the rotating table, so that both views of the liquid bridge contour, say frontal view and lateral one, are recorded at the same time. However, leaving apart geometrical and cleaning constraints, with the available optics for the CCD camera there were some problems to keep both images in focus; thus only a liquid bridge contour was recorded for each angle β_n, and the hypothesis that each liquid bridge interface can be identified by the images recorded at angles β_n and $\beta_n + \pi/2$ was made.

Seven nominal values of the tilt angle ($\varphi_n = 0°$, 13°, 26°, 40°, 50°, 67°, and 90°) and seven nominal values of the rotation angle ($\beta_n = 0°$, 15°, 30°, 45°, 60°, 75°, and 90°) were considered. For each orientation of the liquid bridge axis (defined by the angles φ_n and β_n) the process described above was repeated 10 times. As previously stated the aim of these experiments was to measure the steady Bond numbers corresponding to the axial and lateral components of the acceleration acting on the liquid bridge as well as the direction in which it acts in each case or, in other words, the angles φ and β corresponding to each experiment. To do this the process of the analysis of the experimental results has been done in two steps. The first step is to calculate, from each pair of images identified by some nominal angles β_n and $\beta_n + \pi/2$, the unknown angle β. Once β is calculated and the direction in which radial acceleration acts is known, axial and lateral Bond numbers are calculated by fitting eq. (6) to experimental liquid bridge contours, from which the angle φ is obtained.

The direction of the lateral acceleration is calculated as follows. Let us consider two liquid bridge contours corresponding to the angles β_n and $\beta_n + \pi/2$. Such contours define 4 points on each section parallel to the disks of the liquid bridge. Assuming that the liquid bridge section is circular, these points define the position of the center of the section with respect to the liquid bridge axis or, in other words, the direction in which lateral acceleration is acting, as well as an estimate of the value of the lateral Bond number, B_l. In effect, according to eq. (6) at $z = 0$ the distance between the liquid bridge axis and the center of the section is

$$d(0) = \frac{1}{2}\left[\Lambda^2 + N(3 - 3\cos(\Lambda) - \Lambda\sin(\Lambda) - \frac{1}{2}\Lambda^2\cos(\Lambda))v\right]B_l, \tag{17}$$

where $d(0)$ has been made dimensionless with R_0 and $N = \Lambda(\sin(\Lambda) - \Lambda\cos(\Lambda))^{-1}$. Therefore, eq. (17) allows us to estimate the value of B_l provided the volume $v = V - 1$ is known. In the experiments is was $v \approx 0$, so that, in a first approximation, $B_l = 2d(0)/\Lambda^2$.

Before pursuing further it would be convenient to have an idea about the errors involved in the determination of both $d(0)$ and β. Obviously, since liquid-bridge contours are determined with some error (*Perales* and *Meseguer* [9]), there will be some uncertainty in determining the position of the centers of the different liquid-bridge cross-sections. Let ε be the error in the position of the center of the middle cross-section. Then the distance between the liquid-bridge

Table 1. Variation of the measured Bond number, B_l, with the nominal rotation angle, β_n, and the nominal tilt angle, φ_n

φ_n \ β_n	0°	15°	30°	45°	60°	75°	90°
0				0.0232 ±0.0001			
13°	0.0226 ±0.0001	0.0227 ±0.0001	0.0237 ±0.0001	0.0231 ±0.0001	0.0236 ±0.0001	0.0235 ±0.0001	0.0234 ±0.0001
26°	0.0231 ±0.0001	0.0232 ±0.0001	0.0235 ±0.0002	0.0236 ±0.0001	0.0237 ±0.0001	0.0237 ±0.0001	0.0237 ±0.0001
40	0.0230 ±0.0001	0.0234 ±0.0001	0.0234 ±0.0001	0.0234 ±0.0001	0.0236 ±0.0001	0.0238 ±0.0001	0.0233 ±0.0001
54	0.0233 ±0.0002	0.0233 ±0.0002	0.0236 ±0.0001	0.0235 ±0.0001	0.0230 ±0.0001	0.0231 ±0.0002	0.0229 ±0.0002
67	0.0235 ±0.0002	0.0234 ±0.0002	0.0234 ±0.0003	0.0235 ±0.0001	0.0235 ±0.0002	0.0231 ±0.0001	0.0235 ±0.0002
90°	0.0235 ±0.0002	0.0230 ±0.0002	0.0237 ±0.0001	0.0233 ±0.0003	0.0231 ±0.0003	0.0232 ±0.0002	0.0232 ±0.0003

Table 2. Variation of the tilt angle, φ, with the nominal rotation angle, β_n, and the nominal tilt angle, φ_n

φ_n \ β_n	0°	15°	30°	45°	60°	75°	90°
0°				1.9° ±1.6			
13	13.3° ±0.6	13.1° ±0.1°	13.4° ±0.5	13.5° ±0.4°	12.4 ±0.6°	13.4° ±0.6°	12.7° ±0.5°
26	25.4° ±0.6°	25.2° ±0.5	27.0° ±0.6	26.0° ±0.5°	25.3° ±0.3°	25.1° ±0.6°	24.7° ±0.5°
40	40.1 ±0.4°	40.0° ±0.4°	40.3° ±0.6	40.1° ±0.3°	40.6° ±0.6°	40.1° ±0.3°	39.6° ±0.3°
54	52.6° ±0.4°	53.1° ±0.4°	53.7° ±0.3°	53.4° ±0.2°	53.1° ±0.2°	53.6° ±0.4°	52.9° ±0.3°
67°	66.7° ±0.2°	65.7° ±0.6°	66.4° ±0.4°	65.7° ±0.2°	65.8° ±0.2°	64.9° ±0.4°	64.8° ±0.2°
90°	90.5° ±0.2°	91.0° ±0.3°	90.7 ±0.2°	89.9° ±0.2°	89.5° ±0.1°	89.8° ±0.1°	90.0° ±0.3°

axis and the center of this cross-section will be $d(0) \pm \varepsilon$, and the rotation angle will be $\beta \pm \Delta\beta$, where

$$\Delta\beta = \sin^{-1}(\varepsilon/d(0)), \quad \varepsilon \leq d(0). \tag{18}$$

According to this last expression the error in β increases as $d(0)$ decreases. It is obvious that to use this method to measure β becomes unacceptable when $d(0) \sim \varepsilon$. In the experiments described here it was $\varepsilon = 0.0016$.

Once β is known the lateral and axial Bond numbers, B_l and B_a, respectively, are calculated, from which the angle $\varphi = \tan^{-1}(B_l/B_a)$ and the Bond number $B = (B_l^2 + B_a^2)^{1/2}$ are obtained.

The measured values of B, φ, and β as functions of the nominal values φ_n and β_n are shown in tables 1–3, respectively. It can be seen that all measured values of the Bond number are in the range $B = 0.0232 \pm 0.0006$, the average being $B = 0.0233$. That means that the maximum difference of measured Bond number from the average is 2.5%, no matter what the values of φ_n and β_n are. From table 1 it seems that there is no dependence of the value of measured Bond number on the tilt angle or on the notation angle. An explanation for the differences between the experimental results from one experimental sequence to any other may be the variation of the surface tension of the working fluid (distilled water). In effect, for $\varrho = 10^3\ \mathrm{kg \cdot m^{-3}}$, $g = 9.81\ \mathrm{m \cdot s^{-2}}$ and $R_0 = 0.41 \cdot 10^{-3}$ m, the value of the surface tension corresponding to $B = 0.0232$ is $\sigma = 0.071\ \mathrm{N \cdot m^{-1}}$, which is practically the nominal value of the surface tension of water. But the surface tension of water is known to decrease with interface contamination. Other liquids less sensitive to interface contamination, such as silicone oils, were considered as candidates to be used as working fluids.

Table 3. Variation of the rotation angle, β, with the nominal rotation angle, β_n, and the nominal tilt angle, φ_n

φ_n \ β_n	0°	15°	30°	45°	60°	75°	90°
13°	3.4° ±3.8°	14.7° ±5.0°	29.0° ±3.5°	45.3° ±5.2°	65.9° ±5.9°	76.5° ±6.5°	89.0° ±7.1°
26°	−0.2° ±3.5°	14.0° ±1.6°	30.0° ±2.2°	46.8° ±2.3°	60.0° ±2.9°	73.7° ±3.6°	89.0° ±2.6°
40°	2.9° ±1.6°	15.7° ±2.6°	31.1° ±1.4°	45.9° ±1.2°	59.3° ±1.6°	74.9° ±0.6°	89.1° ±1.6°
54°	1.8° ±1.1°	15.8° ±1.0°	30.4° ±1.6°	47.0° ±1.1°	59.2° ±1.2°	74.7° ±1.6°	90.5° ±1.0°
67°	1.9° ±1.0°	15.6° ±1.3°	29.8° ±1.7°	45.9° ±1.0°	59.5° ±1.4°	74.1° ±1.4°	89.5° ±1.2°
90°	2.5° ±1.0°	17.3° ±1.2°	32.7° ±1.0°	45.2° ±1.6°	59.9° ±0.9°	73.1° ±1.5°	89.4° ±0.6°

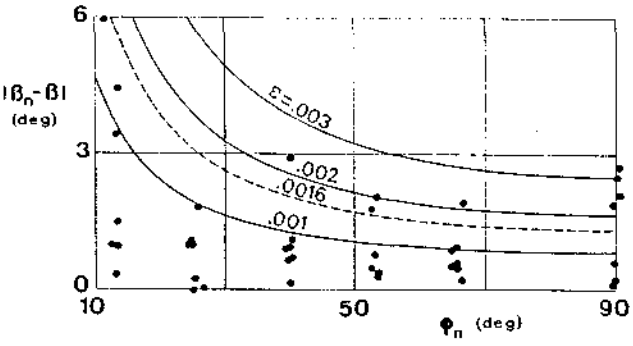

Fig. 5. Variation with the measured tilt angle, φ_n, of the difference $\Delta\beta = |\beta_n - \beta|$ where β_n is the nominal value of the measured angle β. The symbols represent experimental results whereas the solid lines correspond to theoretical predictions using eq. (18)

Such liquids were not used because, except in the case of water, severe problems to keep the liquid bridge interface anchored to the edges of the disks were faced, not to mention the cleaning problem associated with these liquids.

From tables 2 and 3 one can notice that the error in the determination of the direction of the lateral component of the acceleration, the rotation angle β, is much larger than the error in the angle φ. This is because of the different methods used to determine each one of the angles. In the case of β only 4 points of the liquid bridge contours are used, whereas for the measurement of φ the whole liquid bridge contours are used. Furthermore, as has been previously stated, the measured values of β become more scattered as the tilt angle φ_n decreases, as pointed out in fig. 5, where the modulus of the difference between the nominal and measured values of the rotation angle, $|\beta_n - \beta|$, versus the measured tilt angle, φ, is depicted. In effect, since the value of the lateral Bond number is proportional to $\sin(\varphi)$, $B_l = B\sin(\varphi)$, the distance between the axis of the disks and the liquid-bridge section corresponding to $z = 0$, $d(0)$, will be $d(0) = \frac{1}{2}\Lambda^2 B\sin(\varphi)$. Therefore, according to eq. (18) the accuracy in the measurement of the rotation angle β will decrease as the tilt φ decreases. In fig. 5 the theoretical estimation of the error in the measurement of the rotation angle, $\Delta\beta$, resulting from (18), is plotted.

In conclusion, a method to measure both the modulus and the direction of the steady acceleration acting on a liquid column has been presented. Although the method requires some additional refinements, experimental results seem to indicate that a liquid bridge can be used as a fluid accelerometer to measure very small steady accelerations like the ones appearing in space laboratories, although their use as accelerometers would require a considerable additional effort.

Acknowledgments

This work has been supported by the Spanish Comisión Interministerial de Ciencia y Tecnología (CICYT) and is part of a more general endeavour for the study of fluid physics and materials processing under microgravity (Project No. ESP95-0029).

Appendix

The solutions of the different sets of order ε_i problems, eqs. (7)–(10), and order $\varepsilon_i\varepsilon_j$ problems, eqs. (11)–(14), are the following:

$$f_1 = \frac{1}{2}N(\cos(z) - \cos(\Lambda)), \quad N = \frac{\Lambda}{\sin(\Lambda) - \Lambda\cos(\Lambda)}. \tag{A.1}$$

$$f_2 = z - \Lambda\frac{\sin(z)}{\sin(\Lambda)}. \tag{A.2}$$

$$f_3 = \frac{\sin(z)}{\sin(\Lambda)}. \tag{A.3}$$

$$f_4 = \frac{1}{2}(\Lambda^2 - z^2)\cos(\theta - \alpha). \tag{A.4}$$

$$f_5 = \frac{z}{\Lambda}\cos(\theta). \tag{A.5}$$

$$f_{11} = T_{11}(z) - T_{11}(\Lambda),$$

$$T_{11} = \frac{1}{4}N^2\left\{\frac{1}{2}\sin^2(z) + \cos(\Lambda)[(2 - N\Lambda\sin(\Lambda))\cdot\cos(z) - z\sin(z)]\right\}. \tag{A.6}$$

$$f_{12} = T_{12}(z) - T_{12}(\Lambda)\frac{\sin(z)}{\sin(\Lambda)},$$

$$T_{12}(z) = \frac{1}{4}N\left\{\frac{1}{2}z^2\sin(z) - 2z\cos(\Lambda) + \frac{\Lambda}{\sin(\Lambda)}\cos(z)\sin(z) - \frac{\Lambda\cos(\Lambda)}{\sin(\Lambda)}z\cos(z)\right\}. \tag{A.7}$$

$$f_{13} = T_{13}(z) - T_{13}(\Lambda)\frac{\sin(z)}{\sin(\Lambda)},$$

$$T_{13}(z) = \frac{N\cos(z)}{4\sin(\Lambda)}(z\cos(\Lambda) - \sin(z)). \tag{A.8}$$

$$f_{14} = [T_{14}(z) - T_{14}(\Lambda)]\cos(\theta - \alpha),$$

$$T_{14}(z) = \frac{1}{4}N\left\{z\sin(z) + 3\cos(z) + \frac{1}{2}z^2\cos(\Lambda)\right\}. \tag{A.9}$$

$$f_{15} = \frac{1}{4\Lambda}N\left\{\frac{z}{\Lambda}\sin(\Lambda) - \sin(z)\right\}\cos(\theta). \tag{A.10}$$

$$f_{22} = T_{22}(z) - T_{22}(\Lambda),$$

$$T_{22}(z) = \frac{\Lambda}{2\sin(\Lambda)}(4 - \Lambda^2 + z^2)\cos(z) + \frac{\Lambda^2}{2\sin^2(\Lambda)}\cos^2(z) + z^2. \tag{A.11}$$

$$f_{23} = T_{23}(z) - T_{23}(\Lambda),$$

$$T_{23}(z) = -\frac{1}{4\sin(\Lambda)}\left[(4 - \Lambda^2 + z^2 - 2N\Lambda\sin(\Lambda))\cos(z) + \frac{2\Lambda}{\sin(\Lambda)}\cos^2(z)\right]. \tag{A.12}$$

$$f_{24} = \left[T_{24}(z) - T_{24}(\Lambda)\frac{z}{\Lambda}\right]\cos(\theta - \alpha),$$

$$T_{24}(z) = \frac{\Lambda}{2\sin(\Lambda)}(z\cos z - 3\sin(z)). \tag{A.13}$$

$$f_{25} = [T_{25}(z) - T_{25}(\Lambda)] \cos(\theta),$$

$$T_{25}(z) = \frac{-1}{2\Lambda}\left(\frac{1}{2}z^2 + \frac{\Lambda}{\sin(\Lambda)}\cos(z)\right). \tag{A.14}$$

$$f_{33} = T_{33}(z) - T_{33}(\Lambda),$$

$$T_{33}(z) = \frac{\cos^2(z)}{2\sin^2(z)} - \frac{1}{2}N\cos(z). \tag{A.15}$$

$$f_{34} = -\frac{1}{\Lambda}f_{24}. \tag{A.16}$$

$$f_{35} = \frac{1}{2\Lambda\sin(\Lambda)}(\cos(z) - \cos(\Lambda)). \tag{A.17}$$

$$f_{44} = \frac{1}{16}\left\{(z^2 - \Lambda^2) + 4z^2 + \frac{3}{8} - \left(4\Lambda^2 + \frac{3}{8}\right)\frac{\cosh(\sqrt{3}z)}{\cosh(\sqrt{3}\Lambda)}\right\}$$

$$\cdot \cos(2(\theta - \alpha)) + T_{44}(z) - T_{44}(\Lambda),$$

$$T_{44}(z) = \frac{1}{2}N\Lambda^2\cos(z) - \frac{z^2}{8}\left(\frac{1}{2}z^2 - \Lambda^2 - 6\right). \tag{A.18}$$

$$f_{45} = \frac{1}{8\Lambda}\left\{(\Lambda^2 - 2)z - z^3 + 2\Lambda\frac{\sinh(\sqrt{3}z)}{\sinh(\sqrt{3}\Lambda)}\right\}\cos(2\theta - \alpha)$$

$$+ T_{45}(z) - T_{45}(\Lambda)\frac{\sin(z)}{\sin(\Lambda)},$$

$$T_{45}(z) = \frac{\cos(\alpha)}{8\Lambda}[z^2 - (\Lambda^2 + 6)z]. \tag{A.19}$$

$$f_{55} = \frac{1}{4\Lambda^2}\left\{\left(z^2 + 1 - \frac{\cosh\sqrt{3}z}{\cosh\sqrt{3}\Lambda}\right)\cos(2\theta) - z^2\right\}. \tag{A.20}$$

References

1 *Meseguer, J., Sanz, A.:* Numerical and Experimental Study of the Dynamics of Axisymmetric Liquid Bridges. J. Fluid Mech., vol. 153, p. 83 (1985)

2 *Meseguer, J., Mayo, L. A., Llorente, J. C., Fernández, A.:* Experiments with Liquid Bridges in Simulated Microgravity. J. Crystal Growth, vol. 73, p. 609 (1985)

3 *Pearles, J. M., Meseguer, J., Martínez, I.:* Minimum Volume Stability Limits of Axisymmetric Liquid Bridges Subject to Steady Axial Acceleration. J. Crystal Growth, vol. 110, p. 855 (1991)

4 *Martínez, I.:* Stability of Liquid Bridges – Results of SL-D1 Experiment. Acta Astronautica, vol. 15, p. 449 (1987)

5 *Coriell, S. R., Hardy, S. C., Cordes, M. R.:* Stability of Liquid Zones. J. Colloid Interface Sci., vol. 60, p. 126 (1977)

6 *Perales, J. M.:* Non-Axisymmetric Effects on Long Liquid Bridges. Acta Astronautica, vol. 15, p. 561 (1987)

7 *Chen, H., Saghir, M. Z.:* Nonaxisymmetric Equilibrium Shapes of the Liquid Bridge. Microgravity sci. technol., vol. 7, p. 12 (1994)

8 *Laverón-Simavilla, A., Perales, J. M.:* Equilibrium Shapes of Non-Axisymmetric Liquid Bridges of Arbitrary Volume in Gravitational Fields and Their Potential Energy. Phys. Fluids, vol. 7, p. 1204 (1995)

9 *Pearles, J. M., Meseguer, J.:* Theoretical and Experimental Study of the Vibration of Axisymmetric Viscous Liquid Bridges. Phys. Fluids A, vol. 4, p. 1110 (1992)